MIT Libraries | DSpace@MIT

MIT Open Access Articles

Mutation of p107 exacerbates the consequences of Rb loss in embryonic tissues and causes cardiac and blood vessel defects

Massachusetts Institute of Technology

Mutation of *p107* exacerbates the consequences of *Rb* loss in embryonic tissues and causes cardiac and blood vessel defects

Seth D. Berman[a], Julie C. West[a], Paul S. Danielian[a], Alicia M. Caron[a], James R. Stone[b], and Jacqueline A. Lees[a,1]

[a]David H. Koch Institute for Integrative Cancer Research at MIT, Cambridge, MA 02139; and [b]Massachusetts General Hospital, Boston, MA 02114

The retinoblastoma tumor-suppressor protein, pRb, is a member of the pocket protein family that includes p107 and p130. These proteins have well-defined roles in regulating entry into and exit from the cell cycle and also have cell cycle–independent roles in facilitating differentiation. Here we investigate the overlap between pocket protein's function during embryonic development by using conditional mutant alleles to generate *Rb;p107* double-mutant embryos (DKOs) that develop in the absence of placental defects. These DKOs die between e13.5 and e14.5, much earlier than either the conditional *Rb* or the germline *p107* single mutants, which survive to birth or are largely viable, respectively. Analyses of the e13.5 DKOs shows that *p107* mutation exacerbates the phenotypes resulting from pRb loss in the central nervous system and lens, but not in the peripheral nervous system. In addition, these embryos exhibit novel phenotypes, including increased proliferation of blood vessel endothelial cells, and heart defects, including double-outlet right ventricle (DORV). The DORV is caused, at least in part, by a defect in blood vessel endothelial cells and/or heart mesenchymal cells. These findings demonstrate novel, overlapping functions for pRb and p107 in numerous murine tissues.

cell cycle | heart | p107 | retinoblastoma

The human retinoblastoma gene, *RB-1*, which encodes pRB, was the first identified tumor suppressor. pRB belongs to the pocket protein family that includes p107 and p130 (1). All 3 pocket proteins have some ability to promote G_0/G_1 arrest, in part through repression of E2F-responsive genes that encode key regulators of cell proliferation (1). But the mechanisms of action of these proteins have significant differences, with p107 and p130 being more similar to each other than to pRB (1). First, the pocket proteins target different subsets of the E2F family. p107 and p130 bind specifically to the repressive E2Fs, E2F4 and E2F5, and the resulting complexes bind and repress E2F-responsive promoters in G_0/G_1 cells via recruitment of histone deacetylases. pRB regulates E2F4 in a similar manner to p107 and p130, but it also binds the activating E2Fs, E2F1, 2, 3A and 3B during G_1 and inhibits their transcriptional activity. Mitogenic signaling induces phosphorylation of pRB, p107, and p130 by the cyclin–dependent kinases. This induces dissociation of the pocket protein–E2F complexes, thereby relieving repression and allowing the activating E2Fs to promote transcription. The second distinct feature of the pocket proteins is that pRB associates with various transcription factors that drive tissue-specific differentiation, but p107 and p130 do not seem to share this function. Finally, there is a fundamental difference in the tumor-suppressive properties of pRB versus p107 and p130: *RB-1* is inactivated in approximately one-third of all human tumors, whereas *p107* and *p130* are rarely disrupted. This has led to intense interest in establishing the relative roles of the pocket proteins in vivo.

Mouse models have been a key tool in probing the pocket proteins' tumor-suppressive properties. $Rb^{+/-}$ mice develop tumors with near-complete penetrance, but inactivation of *p107* or *p130* does not yield tumors (2–4). However, chimeric mouse studies show that a loss of both *Rb* and *p107* or *Rb* and *p130* causes a broader spectrum of tumors than that resulting from mutation of *Rb* alone (5). Thus, p107 and p130 can substitute for pRB in suppressing tumor formation in some tissues. Germline mutant mice also have yielded key insights into the pocket proteins' roles in normal development (6). In mixed C57BL/6 × 129/Sv and pure 129/Sv backgrounds, $p107^{-/-}$ and $p130^{-/-}$ mutant mice are largely viable and have few or no defects (3, 4). Even the combined mutation of *p107* and *p130* yields live-born mice in which most tissues appear normal (4); the few exceptions include defects in long-bone development, abnormal epidermal differentiation, and early neonatal lethality of $p107^{-/-};p130^{-/-}$ mice (4, 6). In stark contrast, in the same genetic backgrounds, the $Rb^{-/-}$ mice die in mid-gestation (between e13.5 and e15.5), with ectopic proliferation and apoptosis in the central nervous system (CNS), peripheral nervous system (PNS), and lens (2, 7). These $Rb^{-/-}$ mice also have an erythroid defect that was initially thought to account for their death (8). Early studies showed that $Rb^{-/-};p107^{-/-}$ embryos died only slightly earlier (1–2 days) than the *Rb* germline mutants (3). This suggested that little functional overlap exists between pRb and p107 and supported the view of *Rb* as the most important pocket protein in vivo. But later studies showed that the mid-gestational lethality of the germline $Rb^{-/-}$ embryos is due to poor placental function (9). Indeed, $Rb^{-/-}$ embryos survive to birth when provided with a wild-type placenta. Although ectopic proliferation still occurs in the lens, CNS, and PNS, the apoptosis is largely suppressed, suggesting that this is due in large part to placental insufficiency (9). The erythroid defect is also reduced but not fully rescued, indicating that this has both cell and noncell autonomous origins (8). Finally, this and other mouse models revealed a key role for *Rb* in the development of skeletal muscle, bone, and skin and intestinal epithelia (6, 10, 11). Many tissues develop completely normally in the absence of pRB, however. Given this revised appreciation of the developmental role of *Rb*, we used conditional mice to examine the relationship between *Rb* and *p107* when embryos develop in the context of a wild-type *Rb* placenta.

Results

$Rb^{c-/c-};p107^{-/-};Mox2^{+/Cre}$ Double-Mutant Embryos Die During Mid-Gestation. To assess the potential overlap between *Rb* and *p107* in embryos developing without placental deficiency, we crossed germline *p107* mutants (12) with lines carrying conditional alleles of *Rb* ($Rb^{c/c}$; ref. 12) or the *Mox2-Cre* transgene

Table 1. DKO's ($Rb^{c-/c-};p107^{-/-};Cre^+$) die between e13.5 and e14.5

Genotype*	p107$^{+/-}$ Rb$^{+/c}$Cre$^-$	p107$^{+/-}$ Rb$^{+/c}$Cre$^+$	p107$^{+/-}$ Rb$^{c/c}$Cre$^-$	p107$^{+/-}$ Rb$^{c-/c-}$Cre$^+$	p107$^{-/-}$ Rb$^{+/c}$Cre$^-$	p107$^{-/-}$ Rb$^{+/c}$Cre$^+$	p107$^{-/-}$ Rb$^{c/c}$Cre$^-$	p107$^{-/-}$ Rb$^{c-/c-}$Cre$^+$	Total
Obs e13.5	30	35	19	13	25	26	18	25	191
Exp e13.5	23.875	23.875	23.875	23.875	23.875	23.875	23.875	23.875	191
Obs e14.5	12	11	13	12	14	12	10	9 (7)†	93
Exp e14.5	11.625	11.625	11.625	11.625	11.625	11.625	11.625	11.625	93

*Mice were generated from crosses of $Rb^{+/c};p107^{+/-};Mox2^{+/Cre}$ males with $Rb^{c/c};p107^{-/-}$ females.
†Number in parentheses indicates dead embryos.

($Mox2^{+/Cre}$; ref. 13) to generate 4 test genotypes: $Rb^{+/c};p107^{+/-}$ (control), $Rb^{+/c};p107^{-/-}$ (p107 mutant), $Rb^{c-/c-};p107^{+/+};Mox2^{+/Cre}$ (Rb mutant), and $Rb^{c-/c-};p107^{-/-};Mox2^{+/Cre}$ (DKO). The *Mox2-Cre* strain expresses the Cre recombinase specifically in the embryo proper, beginning around e6.5 (13), and thus the extraembryonic tissues are *Rb* wild-type irrespective of the embryo's genotype. Accordingly, the placental tissues were found to be completely normal in the *Rb* mutants, as well as in all other genotypes studied [supporting information (SI) Fig. S1]. Having verified placental integrity, we next examined the embryos' lifespan. As reported previously (9), the presence of a wild-type placenta allowed *Rb* mutant embryos to survive to birth. In contrast, viable DKOs were not observed at this time point (data not shown). Timed pregnancies showed that DKOs were present at the expected Mendelian ratio at e13.5 (Table 1) and were alive, as judged by the presence of a heartbeat. DKO embryos were present but mostly dead at e14.5 (Table 1) and were absent at later time points. These results indicate that loss of *p107* shortens the lifespan of *Rb* mutant embryos from birth to between e13.5 and 14.5.

***p107* Loss Exacerbates Proliferation and Apoptosis Defects in the CNS and Lens of *Rb* Mutants.** We next explored whether *p107* loss alters the known phenotypes of *Rb* mutants. First, we screened the CNS, PNS, and ocular lens of viable e13.5 embryos for proliferation and apoptosis (Fig. 1*A* and Fig. S2). As expected (9), the *Rb* mutants displayed a significantly higher level of proliferating cells in the CNS, PNS, and lens than either the control or *p107* mutants (which were indistinguishable from one another). Loss of *Rb* also caused a low but significant level of apoptosis in all 3 tissues. The additional loss of *p107* had no detectable effect on

either the proliferation or apoptosis defects in the dorsal root ganglia of the PNS of *Rb* mutants. In contrast, proliferation and apoptosis levels were significantly higher in the hindbrain (CNS) and the ocular lens of DKOs versus *Rb* mutants. In addition, sporadic apoptosis was detected in the liver and skeletal muscle of DKOs but not of other genotypes (data not shown). Together, our data indicate that p107 is able to substitute, either partially or fully, for critical pRB functions in the CNS, ocular lens, liver, and skeletal muscle.

Because *Rb* inactivation is known to disrupt erythroid development (8), we also examined the fetal erythroid cells present in the placental sections. We could not assess enucleation (which is known to be defective in *Rb* mutants), because the erythroid cells were mostly nucleated at e13.5; however, we could screen for erythroid abnormalities, such as irregularly shaped, multiple, or fragmented nuclei. This analysis revealed the expected spectrum of erythroid defects in the *Rb* mutant and showed that the percentage of affected cells was not altered in the DKOs (Fig. S3). Thus, at least at this developmental stage, *p107* does not synergize with *Rb* in fetal erythroid development.

DKO Embryos Exhibit Edema and Severe Heart Defects. The analysis of e13.5 and e14.5 embryos also revealed macroscopic phenotypes specific to the DKOs. First, the yolk sacs of DKOs were bloated and abnormally large, and some (although not all) were abnormally pale (Fig. 2; data not shown). Compared with all

Fig. 1. Mutation of *p107* exacerbates the proliferative and apoptotic defects observed in the CNS and lens, but not the PNS, of $Rb^{c-/c-}$ embryos. Average percentage of BrdU- and TUNEL-positive nuclei in indicated tissues from e13.5 embryos ($n \geq 3$ for each genotype). Error bars represent 1 standard deviation. The asterisks denote statistical significance ($P < .05$) compared with controls and $p107^{-/-}$ (*) or $Rb^{c-/c-}$ (**).

Fig. 2. DKOs display several abnormal macroscopic phenotypes. (*A*) At e13.5, the yolk sacs of DKOs are enlarged (arrow) compared with other genotypes. (*B*) DKO embryos have a bloated midsection, a more severely hunched neck, and occasional hemorrhaging (arrow). (*C*) Edema (arrow) in sagittal sections of the DKO embryos. (Magnification: X4.) (Scale bar: 500 μm.) H, heart; L, liver.

GENETICS

Pulmonary Valve · **Aortic Valve**

CT · p107 · Rb · DKO

Normal PV · DORV PV · Normal AV · DORV AV

Fig. 3. DKO hearts display DORV. Transverse section of e13.5 embryonic hearts showing the pulmonary and aortic valves. (Scale bar: 500 μm.) Schematic diagrams show normal and DORV hearts from both views. The DKO hearts exhibit dilated atria, a thin myocardial wall (large arrow) and DORV. The $Rb^{c-/c-}$ hearts show only slightl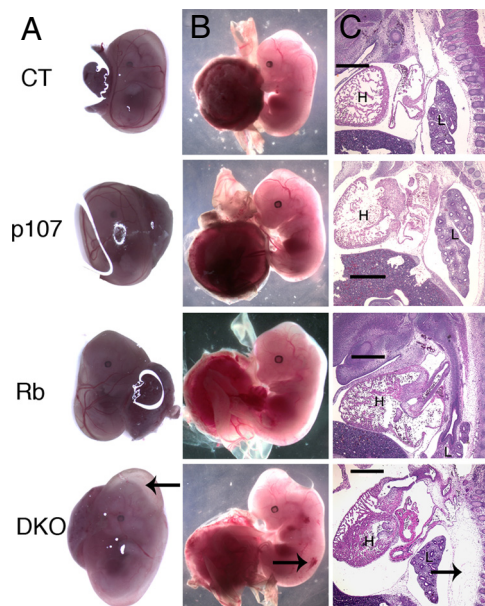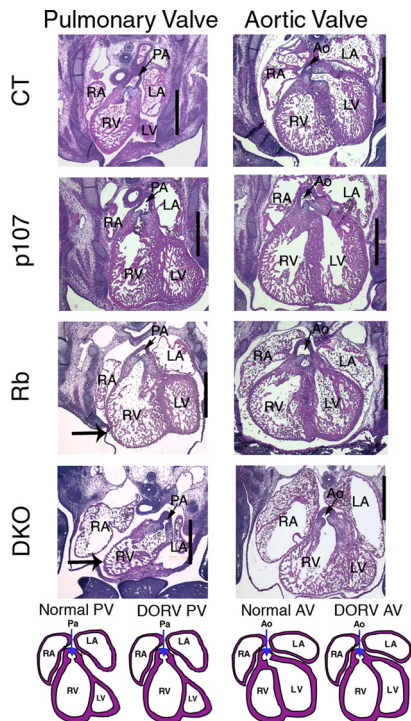y thinner myocardial walls compared with control hearts (large arrow). Ao, aorta and aortic valve; LA, left atrium; LV, left ventricle; RA, right atrium; RV, right ventricle; PA, pulmonary artery and pulmonary valve.

other genotypes, the e13.5 and e14.5 DKOs exhibited a more severely hunched appearance and a bloated midsection, and a subset had hemorrhaging. These phenotypes led us to investigate the embryos in more detail. Sagittal sections revealed severe edema in the vast majority of DKOs examined (10/14 at e13.5; 5/6 at e14.5) that was most prevalent along the backbone but was also seen in the midsection and around the skull (Fig. 2 and data not shown). In contrast, edema was completely absent in the control ($n = 5$ at e13.5; $n = 2$ at e14.5) and p107 mutant ($n = 2$ at e13.5; $n = 4$ at e14.5) embryos and was present only in a much milder form in a subset of the Rb mutants (1/4 at e13.5; 1/2 at e14.5).

There are several known causes of edema, including kidney, lung, and heart dysfunction, as well as anemia. We ruled out kidney and lung dysfunction, because these organs were histologically normal in the DKOs (data not shown) and also are known to be dispensable for fetal development. We next considered erythroid defects and anemia. Although the DKOs had abnormal erythroid cells, the frequency was the same as that seen in nonedematous Rb mutant embryos (Fig. S3). Some DKO yolk sacs were pale, indicating mild anemia, but the DKO embryos showed no evidence of severe anemia (data not shown). Thus, these defects seemed insufficient to explain the edema. Finally, we screened for heart defects, a common cause of edema in humans (14), by comparing serial transverse sections of e13.5 hearts from DKOs with those of other test genotypes (Fig. 3 and data not shown). Control ($n = 6$), p107 ($n = 3$), and Rb ($n = 3$) mutant embryos displayed relatively normal architecture and development of the heart, great arteries (pulmonary artery and aorta), and valves, with the exception of a marginally thinner myocardial wall in the Rb mutants. In contrast, all 7 of the DKOs

CT · p107 · pRb · DKO
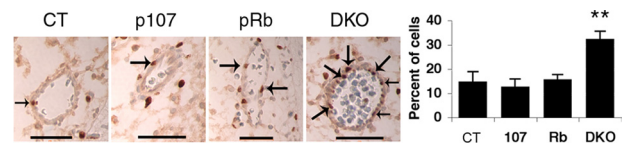
Fig. 4. DKO blood vessels exhibit increased proliferation. BrdU incorporation in blood vessels of e13.5 embryo heads. Arrows indicate positively stained cells. (Scale bar: 50 μm.) Statistical significance is as noted in Fig. 1.

serially examined exhibited double-outlet right ventricle (DORV), in which both the pulmonary artery and the aorta exit from the right ventricle. Some DKOs also displayed dilated atria and thin myocardial walls, while others had atrial and ventricular septum formation defects (data not shown). Because ventricular septum formation is only just completed by e13.5 in wild-type embryos and its timing can vary somewhat, this finding could reflect either a specific septal defect or a subtle developmental delay in the DKOs. Overall, our data indicate that pRb and p107 play overlapping roles in embryonic heart development.

It has been reported that $Rb^{-/-}$ embryonic stem (ES) cells have impaired capacity to induce cardiomyocyte genes and differentiate in vitro (15). Thus, we isolated RNA from the hearts of e13.5 embryos and analyzed the mRNA levels of key cardiac transcription factors and differentiation markers by quantitative RT-PCR (qRT-PCR) (Fig. S4). In contrast to the in vitro ES cell analysis, we found no down-regulation of cardiomyocyte markers in the Rb mutants or DKOs. In fact, several cardiomyocyte markers of the Mesp1/2 pathway (i.e., *Mesp2*, *Nkx2.5*, *Gata4*, and *ANF*) had higher mRNA levels in the DKOs than in the other genotypes. These findings suggest that the heart defects are not due to any general defect or delay in cardiomyocyte differentiation.

p107 is a known E2f target gene, and in some settings pRb loss has been shown to increase p107 mRNA levels, presumably as a direct result of E2f activation (16). This is thought to contribute to p107's ability to compensate for pRb loss. Thus, we investigated whether there was any up-regulation of *p107* mRNA in *Rb* mutant hearts that might contribute to the very modest heart phenotype in *Rb* mutants versus the DKOs. Using qRT-PCR to compare *p107* and *Rb* mRNA levels in the e13.5 hearts of wild-type, *p107*, and *Rb* mutant embryos, we found no detectable increase in *p107* mRNA in the *Rb* mutants (Fig. S4). Together, these data show that pRb plays a key role in heart development in vivo, but that normal levels of p107 can largely substitute for this function, and thus major heart defects occur only after combined loss of pRb and p107.

DORV in the DKOs Is Likely Due To Endothelial or Mesenchymal Cell Defects. Given the relatively normal expression of cardiomyocyte markers in the DKO hearts, we next examined the development of the great arteries and/or other blood vessels. Immunohistochemical analyses of several blood vessel markers, including smooth muscle actin, laminin, and fibronectin, revealed no major disruption of blood vessel differentiation in the DKOs (Fig. S5 and data not shown). Keeping in mind the consequences of pocket protein loss in other tissues, we next examined cellular proliferation and apoptosis. We detected no apoptosis in any blood vessel cells (data not shown) irrespective of genotype; however, we did detect a significant increase in the number of proliferating endothelial cells lining the blood vessels in the DKOs relative to all of the other genotypes ($n = 4$ for each) (Fig. 4). Thus, while the DKO blood vessels display the appropriate differentiation markers, the endothelial cells are undergoing ectopic proliferation. It seems possible that this defect could disrupt development or function of the blood vessels, perhaps by

Fig. 5. *Tie2-Cre* DKO hearts display DORV phenotypes and show increased proliferation of the heart endocardium. (*A* and *B*) Transverse sections of e13.5 *Tie2-Cre* DKOs through the pulmonary valves (*A*) and aortic valves (*B*). Examples of full DORV (*Middle*) and partial DORV (*Bottom*) are shown. (Scale bar: 500 μm.) Abbreviations are as in Fig. 3. (*C* and *D*) Quantification of BrdU-positive (*C*) and TUNEL-positive (*D*) endothelial cells, mesenchymal cells, and cardiomyocytes in the aortic valves from e13.5 *Tie2-Cre* and *Mox2-Cre* models. * and ** denote significant increases (*P* < .02 and < .01, respectively) relative to controls.

interfering with vessel integrity or microvascular stability, thereby contributing to the development of edema and DORV.

To further examine the basis of the heart defect, we crossed *Rb^{c/+};p107^{+/−}* mice with the *Tie2-Cre* mouse strain (17, 18). We selected this model because it expresses Cre recombinase in 2 different locations that could be relevant to the DKO heart defect: all endothelial cells within the embryo, as well as the mesenchymal cells of the developing pulmonary valves, aortic valves, and atrioventricular canal (17, 18). This latter expression seems to result from endothelial–mesenchymal transdifferentiation in the development of both the atrioventricular canal and outflow tract regions (17). We used timed pregnancies to isolate *Tie2-Cre^+* mutants at e13.5. There were no detectable cardiac defects in *Rb^{−/c−};Tie2-Cre^+* embryos or any other control genotypes (*n* ≥ 3 for each class; data not shown). In contrast, of the 7 *Rb^{c−/c−};p107^{−/−};Tie2-Cre^+* embryos (*Tie2-Cre* DKOs) analyzed, 3 exhibited a partial DORV phenotype and 3 displayed full DORV (Fig. 5*A*). Notably, like the *Mox2-Cre* DKOs, the *Tie2-Cre* DKOs died in utero (data not shown). Thus, we conclude that both the heart defect and embryonic lethality of the DKOs results from the loss of pRb and p107 in cells that express *Tie2-Cre*.

We used BrdU incorporation and TUNEL assays to determine the levels of proliferation and apoptosis in the endothelial, mesenchymal, and cardiomyocyte populations in the hearts of e13.5 embryos taken from both the *Tie2-Cre* and *Mox2-Cre* models (*n* ≥ 3 for each genotype) (Fig. 5 *B* and *C* and Fig. S6). This analysis revealed a statistically significant increase in the level of proliferating cells in both models that was specific to the DKO endothelial cells near the aortic valve. We also detected significantly higher levels of apoptosis in the mesenchyme and myocardium of both the DKO and *p107* mutants in the *Mox2-Cre* model, but not in the *Tie2-Cre* model (Fig. 5 *B* and *C* and Fig. S6). Thus, we conclude that elevated apoptosis is not required for DORV to occur in DKOs, although it could contribute to the greater penetrance of the DORV phenotype in the *Mox2-Cre* versus the *Tie2-Cre* DKOs. Taken together, these data suggest that the incorrect positioning of the aorta, and hence the resulting DORV, is correlated with and likely due primarily to ectopic proliferation of the DKO endothelial cells.

Discussion

Our analysis reveals considerable overlap between *Rb* and p107 function during embryogenesis. First, the DKOs die between e13.5 and e14.5, much earlier than either *Rb* or *p107* single mutants, which survive to birth or are largely viable, respectively.

Second, p107 loss exacerbates some, but not all, of the known defects in *Rb*-deficient embryos. Specifically, we found a statistically significant increase in ectopic proliferation and apoptosis in both the CNS and ocular lens of DKOs versus *Rb* mutants, but both genotypes had similar PNS defects. We speculate that the lack of functional overlap in the PNS is due to the poor expression of *p107* in this tissue (19) and/or that proliferation and apoptosis are already maximally induced by the loss of pRb function. Consistent with both of these hypotheses, we found that *Rb* loss yielded a much stronger response in the PNS than in either the CNS or lens with regard to both proliferation (30.8% vs. 9.0% and 21.7%) and apoptosis (26.1% vs. 4.3% and 6.1%) defects. Notably, *p107* inactivation does not alter the erythroid phenotype of e13.5 *Rb* mutants. However, e13.5 tissues that are completely unaffected by *Rb* loss display ectopic proliferation (blood vessels) or apoptosis (liver and skeletal muscle) defects in the DKOs. Thus, we conclude that *p107* can either partially or fully suppress ectopic proliferation and apoptosis in some, but not all, *Rb*-deficient tissues.

Our analyses also revealed gross abnormalities in DKOs that were absent in *Rb* mutants. External examination showed that the yolk sacs of DKOs were enlarged and bloated and that some appeared abnormally pale. Moreover, the DKO embryos exhibited a bloated midsection, and a subset showed hemorrhaging. We believe that all of these abnormalities are caused by edema. We also detected major heart defects in the DKOs, specifically severely dilated atria and thin myocardial walls. Finally, the DKOs exhibited DORV, in which both great arteries (the pulmonary artery and the aorta) originate from the right ventricle. DORV is a clinically important congenital heart defect resulting from various cellular events, including proliferation and migration defects of neural crest cells, delayed or increased apoptosis in the myocardium of the conotruncal area, and faulty left/right signaling (20). We have been able to narrow down the defective cell types that likely underlie the DKO DORV phenotype to the endothelial cells and/or the mesenchymal cells of the pulmonary and aortic valves/atrioventricular canal, where the *Tie2-Cre* is known to be expressed (17, 18). Interestingly, these mesenchymal cells are thought to arise via endothelial to mesenchymal transdifferentiation of a subset of endothelial cells in the vicinity of the cardiac cushion, the future atrioventricular canal and outflow tract (21). Interestingly, we found no impairment in the expression of either blood vessel or cardiac differentiation markers in the DKOs; however, our analysis revealed a significant increase in the percentage of proliferating endothelial cells in both the *Tie2-Cre* and *Mox2-Cre* DKOs. This raises

the possibility that loss of pRb and p107 allows differentiated cells to remain in cycle, as has been reported previously for Rb-deficient hair cells (22).

Apoptosis can play a crucial role in the alignment of the arteries (20). Of note, although increased apoptosis was noted in the myocardium or the mesenchyme in the *Mox2-Cre* DKOs, this did not occur in the *Tie2-Cre* model at e13.5. Thus, abnormal proliferation of the blood vessel and/or heart endothelial cells seems to be sufficient to account for the development of DORV in the DKOs, presumably by disrupting the appropriate positioning of the outflow tract. But elevated apoptosis may be contributing to the greater penetrance of the DORV phenotype in the *Mox2-Cre* versus the *Tie2-Cre* DKOs. It seems unlikely that DORV is the sole cause of the observed embryonic lethality of the DKOs; however, we note that the *Tie2-Cre* DKOs also die in utero. Thus, we conclude that the embryonic lethality results from a defect in one or more of the cell types in which *Tie2-Cre* is expressed. We speculate that the proliferation defect of the endothelial cells may somehow compromise blood vessel function, and that this acts together with the heart defect to cause edema and embryonic lethality.

In conclusion, our analyses demonstrate that pRb and p107 act together to control the proliferation of many embryonic tissues. In particular, we have identified novel, overlapping functions for pRb and p107 in blood vessel endothelium and endocardial cell proliferation, where loss of these proteins results in DORV, a clinically important congenital heart defect. Interestingly, the combined loss of pRB and p130 pocket proteins is known to disrupt cardiomyocyte differentiation and lead to increased heart size (23). The differential ability of *p107* versus *p130* to synergize with *Rb* in heart endothelial cells versus cardiomyocytes likely reflects differences in the expression patterns of *p107* and *p130* during heart development (23). Importantly, ectopic proliferation was observed in all of the tissues affected by the loss of pRb, pRb and p107, or pRb and p130. This strongly suggests that the overlapping role of the pocket proteins largely reflects their shared role in promoting cell cycle exit. We speculate that the ectopic proliferation results, at least in part, from the deregulation of E2F, but this remains to be established. Similarly, we have yet to understand how pocket protein–deficient cells can differentiate and cycle at the same time.

Materials and Methods

Animal Maintenance and Tissue Analysis. The $Rb^{c/c}$, $p107^{-/-}$, *Mox2-Cre*, and *Tie2-Cre* strains have been described previously (12, 13, 18). All mice were crossed in the mixed C57BL/6 $\times$ 129/Sv background for 2 or more generations, and the Cre transgenes were transmitted through the males to avoid germline deletion (18). Pregnant mice were injected with 5 mg/mL of BrdU in PBS (10 μL/g of body weight) 2 hours before tissue harvest. Embryos were fixed in 4% paraformaldehyde and embedded in paraffin. Serial 6-μm transverse sections were used to analyze the embryonic heart. All other sections were cut sagittally. Immunohistochemical analysis was performed as described previously (11) using antibodies for BrdU (1:50 347580; BD Biosciences), Ki67 (1:50 550609; BD Biosciences), smooth muscle actin (undiluted U7033; DakoCytomation), and laminin and fibronectin (1:100 rabbit Ab, provided by R. Hynes, MIT). TUNEL analysis was performed as directed by the equipment manufacturer (Roche). The percentage of BrdU- or TUNEL-positive cells was assessed by counting all of the large (>8 cell) blood vessels in the field of view (typically multiple vessels) for blood vessel endothelial cells, 50–100 endothelial cells around the aortic valve, and 250–1,000 nuclei for all other tissues. Significance was determined by the 2-sample t test. Error bars in the graphs represent SDs except for blood vessels, where the SEM was used. For qRT-PCR, e13.5 hearts were homogenized in TRIzol (Invitrogen). First-strand cDNA was transcribed from 1 μg of RNA using SuperScript III Reverse Transcriptase (Invitrogen), and qRT-PCR was performed with 20 ng cDNA using SYBR Green (Applied Biosystems). Primer sequences are listed in Table S1.

1. Dimova DK, Dyson NJ (2005) The E2F transcriptional network: Old acquaintances with new faces. *Oncogene* 24:2810–2826.
2. Jacks T, et al. (1992) Effects of an Rb mutation in the mouse. *Nature* 359:295–300.
3. Lee MH, et al. (1996) Targeted disruption of p107: Functional overlap between p107 and Rb. *Genes Dev* 10:1621–1632.
4. Cobrink D, et al. (1996) Shared role of the pRB-related p130 and p107 proteins in limb development. *Genes Dev* 10:1633–1644.
5. Dannenberg JH, Schuijff L, Dekker M, van der Valk M, te Riele H (2004) Tissue-specific tumor-suppressor activity of retinoblastoma gene homologs p107 and p130. *Genes Dev* 18:2952–2962.
6. Wikenheiser-Brokamp KA (2006) Retinoblastoma family proteins: Insights gained through genetic manipulation of mice. *Cell Mol Life Sci* 63:767–780.
7. Macleod KF, Hu Y, Jacks T (1996) Loss of Rb activates both p53-dependent and independent cell death pathways in the developing mouse nervous system. *EMBO J* 15:6178–6188.
8. Macleod KF (2008) The role of the RB tumour-suppressor pathway in oxidative stress responses in the haematopoietic system. *Nat Rev Cancer* 8:769–781.
9. de Bruin A, et al. (2003) Rb function in extraembryonic lineages suppresses apoptosis in the CNS of Rb-deficient mice. *Proc Natl Acad Sci USA* 100:6546–6551.
10. Yang HS, Hinds PW (2007) pRb-mediated control of epithelial cell proliferation and Indian hedgehog expression in mouse intestinal development. *BMC Dev Biol* 7:6.
11. Berman SD, et al. (2008) The retinoblastoma protein tumor suppressor is important for appropriate osteoblast differentiation and bone development. *Mol Cancer Res* 6:1440–1451.
12. Sage J, et al. (2000) Targeted disruption of the three Rb-related genes leads to loss of G1 control and immortalization. *Genes Dev* 14:3037–3050.
13. Tallquist MD, Soriano P (2000) Epiblast-restricted Cre expression in MORE mice: A tool to distinguish embryonic vs. extra-embryonic gene function. *Genesis* 26:113–115.
14. Cho S, Atwood JE (2002) Peripheral edema. *Am J Med* 113:580–586.
15. Papadimou E, Menard C, Grey C, Puceat M (2005) Interplay between the retinoblastoma protein and LEK1 specifies stem cells toward the cardiac lineage. *EMBO J* 24:1750–1761.
16. Sage J, Miller AL, Perez-Mancera PA, Wysocki JM, Jacks T (2003) Acute mutation of retinoblastoma gene function is sufficient for cell cycle re-entry. *Nature* 424:223–228.
17. Kisanuki YY, et al. (2001) *Tie2-Cre* transgenic mice: A new model for endothelial cell-lineage analysis in vivo. *Dev Biol* 230:230–242.
18. Koni PA, et al. (2001) Conditional vascular cell adhesion molecule 1 deletion in mice: Impaired lymphocyte migration to bone marrow. *J Exp Med* 193:741–754.
19. Jiang Z, Zacksenhaus E, Gallie BL, Phillips RA (1997) The retinoblastoma gene family is differentially expressed during embryogenesis. *Oncogene* 14:1789–1797.
20. Obler D, Juraszek AL, Smoot LB, Natowicz MR (2008) Double-outlet right ventricle: Aetiologies and associations. *J Med Genet* 45:481–497.
21. Armstrong EJ, Bischoff J (2004) Heart valve development: Endothelial cell signaling and differentiation. *Circ Res* 95:459–470.
22. Sage C, et al. (2006) Essential role of retinoblastoma protein in mammalian hair cell development and hearing. *Proc Natl Acad Sci USA* 103:7345–7350.
23. MacLellan WR, et al. (2005) Overlapping roles of pocket proteins in the myocardium are unmasked by germ line deletion of p130 plus heart-specific deletion of Rb. *Mol Cell Biol* 25:2486–2497.